A Review of PA-Antenna Co-design

Document status and date:
Published: 31/10/2022

Document Version:
Accepted manuscript including changes made at the peer-review stage

Please check the document version of this publication:

A Review of PA-Antenna Co-design: Direct Matching, Harmonic Tuning and Power Combining

Martijn de Kok[†‡1], Stefania Monni[‡], Marc van Heijningen[‡], Alessandro Garufo[‡], A. Bart Smolders[†] and Ulf Johannsen[†]

[†] Electromagnetics Group, Eindhoven University of Technology, Eindhoven, The Netherlands
[‡] Radar Technology Group, TNO Defense, Safety and Security, The Hague, The Netherlands
[1] m.d.kok@tue.nl

Abstract — This article reviews the current state-of-the-art of active-integrated antennas co-designed with power amplifiers (PAs). Three strategies to improve output power and power-added efficiency are described using examples, namely direct matching between PA and antenna, tuning of harmonic reflections in the antenna, and in-antenna power combining from multiple PAs. An outlook is given on the challenges to be faced in the application of these strategies in wide-scanning phased arrays.

Keywords — Active integrated antennas, power amplifiers, antennas, direct matching, harmonic tuning, power combining.

I. INTRODUCTION

The pursuit of improved performance in wireless communication and sensing devices and the increasing constraint of limited bandwidth availability in the radio frequency (RF) spectrum are pushing developments towards the millimeter-wave (mm-wave) band between 30 and 300 GHz. In automotive radars for example, the 77 GHz band has enabled better accuracy and resolution performance with smaller devices compared to the narrower 24 GHz band [1]. Moreover, a trend can be seen towards sensing devices operating in the D-band beyond 100 GHz, where even wider bandwidths and smaller device sizes can be achieved [2].

The high path losses at mm-wave frequencies impose high effective isotropic radiated power (EIRP) requirements on transmitting wireless systems, leading to a demand for both high antenna gain and transmitted power. As the dimensions of radiating elements scale with the wavelength, a high-gain steerable array can be realized within a relatively small size. However, the dimensions of mm-wave chips and commercial surface-mounted chip packages may not scale equally, leading to a tight area budget for array elements. Furthermore, the achievable performance of power amplifiers (PAs) degrades at increasing frequencies, and material losses increase. RF power losses due to mismatches, interconnects and matching networks can be considered expensive: for high-power radars, power-budget critical satellite payloads, or mass-produced base stations, a few percents increase in power-added efficiency (PAE) can result in a significant reduction of total energy cost, relaxed cooling requirement and increased system lifespan.

This paper provides an overview of active integrated antennas (AIAs) co-designed with PAs in order to optimize output power, efficiency, and device footprint. A distinction is made between three co-design strategies, namely direct matching, harmonic tuning, and power combining. Each strategy is discussed in a separate section in this overview. Key performance indicators from published examples, including RF output power and peak PAE at the PA-AIA interface, are summarized and listed. Most of the open literature deals with standalone antennas and relatively simple amplifiers with few transistors. As novel contribution, in this paper we will discuss the challenges posed by PA-antenna co-design for phased array environments, where aspects such as mutual coupling as a function of scanning play an important role.

II. DIRECT MATCHING

High-power PAs generally require relatively small load resistances at the transistor drain reference plane, whilst most antennas are designed to have higher impedances [3]. Conventionally, PAs are designed with input and output matching circuits to achieve a standardized 50 Ω interface impedances throughout their operating bandwidth. This ensures a degree of modularity and re-usability of PA designs with a wide range of antenna designs, and vice versa. However, when regarding the PA and antenna as one integrated system, this would result in two back-to-back matching networks as depicted in Fig. 1a. This is a sub-optimal solution in terms of compactness and power losses.

Transforming the antenna impedance Z_A to the optimal PA load impedance Z_L could also be achieved directly by a single matching network as in Fig. 1b, resulting in a smaller overall design. As the substrate and ohmic losses in a matching network can be directly linked to its size, this could also lead to lower overall power losses [4]. However, a larger single impedance transformation may limit the transmission bandwidth compared to two smaller transforms.

In Fig. 1c, a direct match between a co-designed PA and antenna is depicted. In this case, the antenna itself is designed to an input impedance corresponding to the desired Z_L. Examples of two different direct-matching strategies are
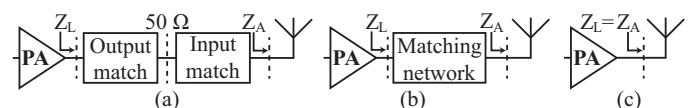

Fig. 1. Schematics of (a) conventional matching with a 50 Ω interface, (b) a single matching network and (c) direct matching between PA and antenna.

Table 1. Examples of direct-matched ([6]-[9]), harmonic-tuned ([10]-[15]), and power-combining ([16]-[21]) AIAs from literature.

Source	Antenna design	f [GHz]	$Z_{A1}(/Z_{A2}/Z_{A3})$ [Ω]	PA class/type [5]	P_{out} [dBm]	PAE_{pk} [%]	BW [%]
[6]	Small patch	0.9	2.8+j0.7	Class A / SOI LDMOS	27.5→31	33→45	1.1
[7]	Small loop	30	5+j500	Class A / GaN HEMT	30	15	-
[8]	Slot	20	17+j46	- / GaN HEMT	24.7	34.8	1.5
[9]	Series-fed patches with PAs in between	5	99-j65	Class A / HJ-FET	≈ 2	19	2
[10]	Rectangular patch shorted at center	2.48	14-j30 / ≈ 0+j30	Class AB/F / GaAs FET	31.6	48→55	-
[11]	Slot with L/C stub	5.4	18.4-j17.5 / 8.5 /800	Class B/F / GaAs FET	26.8→27	64→67.5	9.5
[12]	Dielectric resonator with triple slot feed	14.25	25+j125 / -	- / -	-	-	5
[13]	Square patch with diagonal slots	2.4	47.5-j119 / 0.8-j10.7 / 295-j119	Class B/F / SiGe NPN	11.6→12	62→67	-
[14]	L-shaped microstrip	2.4	22.4+j1.9 / 0.3+j19.4	Class B/F / -	-	62	-
[15]	Triple slot	3.5	12.9-j6.9 / 1.4-j16 / 1011-j204	Class F / GaN HEMT	37.1→38.1	52→65.9	7
[16]	Diff patch	2.5	-	Push-Pull / MESFET	25	55	-
[17]	Proximity-fed Diff patch	2.64	-	Diff / GaAs PHEMT	≈ 22	29	-
[18]	2×2 Diff patch array	45	50	Diff / 45-nm SOI	≈ 28	13.5	≈ 7
[19]	On-chip slot with 4 feeds	59	13 (feed), 52 (PA)	Diff / 45-nm SOI	27.9	23.4	8.5
[20]	Dual-feed loop	28	46	Outphasing / 45-nm SOI	17.1	56 (η_D)	-
[21]	Patch above 4-port slot	3.5	7.5-j21.1 (main) 39.4+j3.3 (auxiliary)	Doherty / GaN HEMT	42.8	61	7

Legend:	Center frequency:	f	Antenna impedance at n^{th} harmonic:	Z_{An}	Differential:	Diff	PA output power:*	P_{out}
	Drain efficiency:*	η_D	-10 dB input-reflection bandwidth:*	BW	Peak PAE:*	PAE_{pk}	*: At $Z_L = Z_A$ interface (Fig.1c)	

listed as [6]–[9] in Table 1. If reported, the improvement with respect to a 50 Ω reference design is indicated by an arrow.

In [6] and [7], electrically small antenna designs are used to achieve very low input impedances and compact form factors. However, in this case there exists a severe trade-off between optimal impedance matching and radiation efficiency [3]. Moreover, electrically small antennas are inherently limited in bandwidth due to the inverse Chu-limit of quality factor.

In [8], a slot antenna was presented that was excited by a bondwire directly connected to the transistor drain. In [9], the radiating elements were also connected directly to the transistor terminals. The equivalent L-C circuit model of a microstrip patch antenna was used as input and output matching networks for a scaleable linear array of AIAs and PAs. Each patch antenna radiates 73% of the input power, and transfers the remaining power to the next PA.

III. Harmonic Tuning

The PAE of a class AB or class B PA can be optimized with open or short terminations of the second and third harmonic components at the transistor output, resulting in class F operation. Although the required harmonic tuning network leads to a somewhat larger and more lossy PA output stage, this downside is often outweighed by the PAE increase.

In [10]–[15] listed in Table 1, several harmonics-tuned AIA designs are presented which allow the removal of such a harmonic tuning network. Not only may this result in a reduction of overall size and losses, it also limits undesired out-of-band radiation. In most designs, the second harmonic and third harmonic load impedances are tuned to an approximate short and approximate open at the transistor reference plane, respectively. A direct impedance match at the fundamental frequency is applied in [11], [14] and [15]. The patch antenna designs presented in [10] and [13] achieve this

by blocking the harmonic surface current paths with shorting vias and slots, respectively. In [11], [12] and [15], tuning stubs or slots are used to achieve the desired harmonic termination. The resulting maximum PAE values (PAE_{pk}) exceed 60% in most designs, and improvements of up to 14 percentage points are reported compared to reference designs.

Most harmonics-tuning AIAs listed in Table 1 are sub-10 GHz designs, bar the theoretic study on a Ku-band dielectric resonator in [12] where only the second harmonic was examined. Accurate phase tuning is required for effective harmonic termination, which increases in challenge as the wavelength decreases. For harmonic tuning to be successful at mm-wave frequencies, the span between transistor drain and antenna interface should be as small as possible and well-modeled in simulations.

IV. Power Combining

Although high-performance III-V semiconductor technologies such as Gallium Nitride (GaN) can achieve much higher power at mm-wave than more conventional silicon-based transistors, the single-transistor power limit remains insufficient for many mm-wave applications. Instead, high-power PAs achieve Watt-level output powers through on-chip or on-board power combining networks as depicted in Fig. 2a [22]. The number of output-stage transistors is limited by practical factors including heat dissipation, die size and combining network losses.

Combining network losses are avoided when combining power from various radiating elements in the air (Fig. 2b), although this results in a directional antenna where power can be considered 'lost' to undesired directions as side-lobes. For situations where a more omnidirectional antenna is required, or in the case of a single array element, combining losses can be avoided by using the antenna itself as power
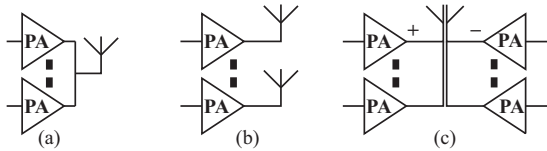
Fig. 2. Schematics of (a) a power combining network, (b) over-the-air combining from multiple radiators and (c) a multi-feed / differential antenna.
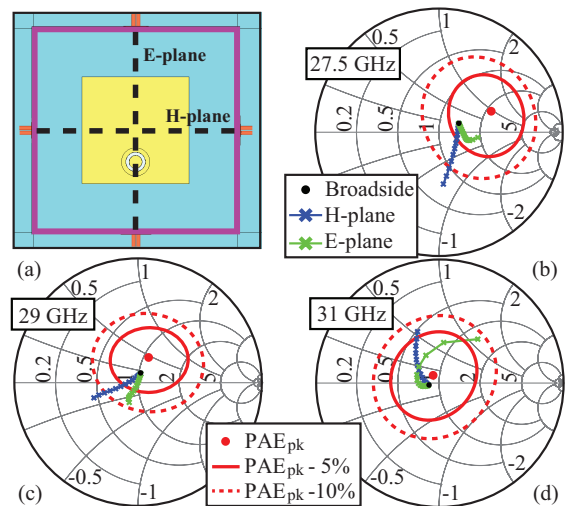

Fig. 3. (a): CST model of a Ka-band stacked patch antenna in an infinite array environment. (b-c): Simulated PAE circles of a reference Ka-band PA at 27.5, 29 and 31 GHz, with the active impedance of the stacked patch under scanning conditions between 0° to 70° from broadside in the E- and H-planes. The reference impedance is 50 Ω.

combiner. As illustrated in Fig 2c, such an antenna can be differential-fed, multi-feed, or a combination of both. Note that this section focuses on integrated PAs and antennas: dedicated power-combining systems such as presented in [23] and [24] are not discussed further for the sake of brevity.

Table 1 lists a number of multi-feed AIA designs from literature, numbered [16]–[21]. Most examples feature a differential-fed antenna element, which is a relatively simple solution to combine twice the number of driving transistors compared to a similar single-ended design. The differential patch antennas presented in [16] and [17] are excited by one transistor per port, connected through inset-feedlines and proximity-coupled lines respectively. In [18], over-the-air combining of four differential-fed patch antennas, for a total of eight PAs, is demonstrated.

Power combining networks scale the antenna impedance, which may be detrimental to high-power mm-wave PAs for which a low load impedance is desired. The slot antenna presented in [19] features both multi-port feeding and power-combining networks: each of the four 13 Ω antenna inputs is fed by four PAs, leading to a perceived load impedance of 52 Ω for each of the 16 PAs.

In [20] and [21], power-combining AIA designs are presented for an outphasing and Doherty PA architecture, respectively. Both types are designed to achieve a good efficiency while operating linearly in back-off. A dual-feed loop antenna has also been demonstrated in combination with an outphasing amplifier in [25]. In the Doherty design, two separate interface impedances must be realized: one for the main and one for the auxilary amplifier.

V. OUTLOOK: PHASED ARRAY APPLICATIONS

All of the AIA designs discussed in this overview consist of a single radiating element, with only the non-scanning patch arrays from [9] and [18] as notable exceptions. In this section, an brief outlook is given on the application challenges of direct matching, harmonic tuning, and in-element power-combining in beamsteering mm-wave phased arrays.

The limited bandwidths of the presented designs in Table 1 may be a severe downside for mm-wave communication and sensing applications. This is especially true in scanning arrays, where the active input impedance can vary significantly with scan angle due to mutual coupling. This phenomenon is illustrated in Fig. 3, where the scanning behavior of a Ka-band stacked patch antenna is shown. Although the patch is matched to around 50 Ω at all three depicted frequencies, the active impedance variations when scanning up to 70° from broadside change significantly with frequency. Moreover,

PA performance varies with frequency as well, as illustrated by the PAE-contours of a reference GaN-based Ka-band PA. The PA has been designed with 50 Ω impedance load (Z_L in Fig. 1) corresponding to the best compromise between optimized output power and PAE. As a result the load value for PAE_{pk} is different than 50 Ω, and changes with frequency. The contours in Fig. 3 show for which complex values of Z_L the PAE decreases to 5% and 10% from PAE_{pk}. It appears that with a 50 Ω load impedance in the considered frequency band the PAE remains within the 5% variation. However, due to the change in active antenna impedance while scanning, and thus in the Z_L seen by the PA, the PAE deteriorates rapidly as in Fig. 3c. In [26], PAE variations of around ten percentage points were also reported due to scanning. These variations make efficient wide-band direct matching between a PA and wide-scanning array element a non-trivial endeavor.

Power-combining array elements also present a number of practical challenges to overcome, stemming from the half-wavelength inter-element spacing requirement to avoid grating lobes. At mm-wave frequencies, the element dimensions may become too small to fit multiple PAs within the unit cell. Moreover, placing PAs in a densely-spaced grid could result in a significant thermal power dissipation in a relatively small area, leading to stringent cooling requirements. A sparse array configuration with fewer higher-powered elements, leading to relaxed area and thermal constraints, could be a promising option in such a case [27]. At sufficiently high output powers, thermals may also constraint the radiating element itself, leading to all-metal designs as presented in [28].

Similarly to the direct-matched and harmonics-tuning AIA concepts, the performance of a power-combining antennas may deteriorate due to scanning. The active impedances can change differently for each port as reported in [28], which will affect the element pattern and radiation efficiency. Whether this

imbalance could be compensated for through the amplitude and phase at the ports, and whether antennas can be designed with better robustness against this effect, are both interesting topics for continued work.

VI. CONCLUSION

This contribution has provided on overview of AIA design techniques including direct matching, antenna-based harmonic tuning and antenna-based power combining based on standalone radiators. Although each active-integration strategy improves upon a given set of figures of merit such as output power and PAE, there are still challenges to be overcome for successful implementation of these strategies in wide-scanning phased-array applications. The most notable of these challenges is the robustness against a varying active impedance under scanning conditions, which could be addressed by investigating techniques aimed at reducing the mutual coupling effect on the array impedance for large scan angles. Moreover research should be pursued in finding the best compromise for the (complex) impedance value at the interface amplifier-antenna, in terms of both PAE and matching for the considered scanning conditions.

ACKNOWLEDGMENT

REFERENCES

[1] K. Ramasubramanian and K. Ramaiah, "Moving from Legacy 24 GHz to State-of-the-Art 77-GHz Radar," *ATZ Elektron Worldw*, vol. 13, p. 46–49, May 2018.

[2] M. de Kok, A. B. Smolders, and U. Johannsen, "A Review of Design and Integration Technologies for D-Band Antennas," *IEEE Open Journal of Antennas and Propagation*, vol. 2, pp. 746–758, 2021.

[3] M. V. Ivashina, "Joint Design and Co-integration of Antenna-IC Systems," in *2019 13th European Conference on Antennas and Propagation (EuCAP)*, 2019, pp. 1–7.

[4] A. Emadeddin and B. L. G. Jonsson, "On Direct Matching and Efficiency Improvements for Integrated Array Antennas," in *2019 International Conference on Electromagnetics in Advanced Applications (ICEAA)*, 2019, pp. 408–411.

[5] I. J. Bahl, *Fundamentals of RF and Microwave Transistor Amplifiers*. Wiley, 2009.

[6] E. Ben Abdallah, A. Giry, S. Bories, D. Nicolas, and C. Delaveaud, "Impact of Small Antenna on Linear Power Amplifier Performance in a Co-design Approach," in *2015 IEEE 13th International New Circuits and Systems Conference (NEWCAS)*, 2015, pp. 1–4.

[7] W.-C. Liao *et al.*, "A Ka-Band Active Integrated Antenna for 5G Applications: Initial Design Flow," in *2018 2nd URSI Atlantic Radio Science Meeting (AT-RASC)*, 2018, pp. 1–4.

[8] W.-C. Liao, R. Maaskant, T. Emanuelsson, V. Vassilev, O. Iupikov, and M. Ivashina, "A Directly Matched PA-Integrated K-Band Antenna for Efficient mm-Wave High-Power Generation," *IEEE Antennas and Wireless Propagation Letters*, vol. 18, no. 11, pp. 2389–2393, 2019.

[9] S. N. Nallandhigal and K. Wu, "Unified and Integrated Circuit Antenna in Front End—A Proof of Concept," *IEEE Transactions on Microwave Theory and Techniques*, vol. 67, no. 1, pp. 347–364, 2019.

[10] V. Radisic, S. T. Chew, Y. Qian, and T. Itoh, "High-efficiency power amplifier integrated with antenna," *IEEE Microwave and Guided Wave Letters*, vol. 7, no. 2, pp. 39–41, 1997.

[11] H. Kim, I.-J. Yoon, and Y. J. Yoon, "A Novel Fully Integrated Transmitter Front-End With High Power-Added Efficiency," *IEEE Transactions on Microwave Theory and Techniques*, vol. 53, no. 10, pp. 3206–3214, 2005.

[12] A. Guraliuc, G. Manara, P. Nepa, G. Pelosi, and S. Selleri, "Harmonic Tuning for Ku-Band Dielectric Resonator Antennas," *IEEE Antennas and Wireless Propagation Letters*, vol. 6, pp. 568–571, 2007.

[13] A. Khoshniat, T. Yekan, R. Baktur, and K. F. Warnick, "Active Integrated Antenna Supporting Linear and Circular Polarizations," *IEEE Trans. Compon. Packag. Manuf. Technol.*, vol. 7, no. 2, pp. 238–245, 2017.

[14] A. Pal *et al.*, "Co-design of an Antenna-Power Amplifier RF Front-end Block Without Matching Network for 2.4 GHz WiFi Application," in *2017 IEEE Radio and Wireless Symposium (RWS)*, 2017, pp. 201–203.

[15] Y. Lu *et al.*, "Seamless Integration of Active Antenna With Improved Power Efficiency," *IEEE Access*, vol. 8, pp. 48 399–48 407, 2020.

[16] W. Deal, V. Radisic, Y. Qian, and T. Itoh, "Integrated-Antenna Push-Pull Power Amplifiers," *IEEE Transactions on Microwave Theory and Techniques*, vol. 47, no. 8, pp. 1418–1425, 1999.

[17] E. Lee, K. M. Chan, P. Gardner, and T. E. Dodgson, "Active Integrated Antenna Design Using a Contact-Less, Proximity Coupled, Differentially Fed Technique," *IEEE Transactions on Antennas and Propagation*, vol. 55, no. 2, pp. 267–276, 2007.

[18] B. Hanafi, O. Gürbüz, H. Dabag, J. F. Buckwalter, G. Rebeiz, and P. Asbeck, "Q-Band Spatially Combined Power Amplifier Arrays in 45-nm CMOS SOI," *IEEE Transactions on Microwave Theory and Techniques*, vol. 63, no. 6, pp. 1937–1950, 2015.

[19] T. Chi, F. Wang, S. Li, M.-Y. Huang, J. S. Park, and H. Wang, "A 60GHz On-Chip Linear Radiator with Single-Element 27.9dBm Psat and 33.1dBm Peak EIRP Using Multifeed Antenna for Direct On-Antenna Power Combining," in *2017 IEEE International Solid-State Circuits Conference (ISSCC)*, 2017, pp. 296–297.

[20] S. Li, T. Chi, H. T. Nguyen, T.-Y. Huang, and H. Wang, "A 28GHz Packaged Chireix Transmitter with Direct on-Antenna Outphasing Load Modulation Achieving 56%/38% PA Efficiency at Peak/6dB Back-Off Output Power," in *2018 IEEE Radio Frequency Integrated Circuits Symposium (RFIC)*, 2018, pp. 68–71.

[21] O. A. Iupikov *et al.*, "A Cavity-Backed Patch Antenna With Distributed Multi-Port Feeding, Enabling Efficient Integration With Doherty Power Amplifier and Band-Pass Filter," *IEEE Transactions on Antennas and Propagation*, vol. 69, no. 8, pp. 4412–4422, 2021.

[22] H. Wang *et al.* (2021) Power Amplifiers Performance Survey 2000-Present (v6). [Online]. Available: https://gems.ece.gatech.edu/PA_survey.html

[23] P. G. Courtney, J. Zeng, T. Tran, H. Trinh, and S. Behan, "120W Ka Band Power Amplifier Utilizing GaN MMICs and Coaxial Waveguide Spatial Power Combining," in *2015 IEEE Compound Semiconductor Integrated Circuit Symposium (CSICS)*, 2015, pp. 1–4.

[24] A. Roev, P. Taghikhani, R. Maaskant, C. Fager, and M. V. Ivashina, "A Wideband and Low-Loss Spatial Power Combining Module for mm-Wave High-Power Amplifiers," *IEEE Access*, vol. 8, pp. 194 858–194 867, 2020.

[25] F. P. van der Wilt, E. Habekotté, and A. B. Smolders, "A Non-Isolated Power-Combining Antenna for Outphasing Radio Transmitters," *IEEE Trans. Antennas Propag.*, vol. 64, no. 2, pp. 761–766, 2016.

[26] W.-C. Liao, T. Emanuelsson, R. Maaskant, A. Vilenskiy, T. Eriksson, and M. V. Ivashina, "Power Efficiency and Linearity of Highly Integrated Transmitting Array Antennas," in *2021 15th European Conference on Antennas and Propagation (EuCAP)*, 2021, pp. 1–5.

[27] M. de Kok, A. B. Smolders, C. Vertegaal, and U. Johannsen, "Active Ka-band Open-Ended Waveguide Antenna with Built-in IC Cooling for Use in Large Arrays," in *Proceedings of the 18th European Radar Conference (EuRAD)*, 2022.

[28] P. M. Kaminski, A. Garufo, E. M. Suijker, R. van Dijk, and S. Monni, "All-Metal Phased Array Antenna Element for High Power Applications," in *Proceedings of the 16th European Conference on Antennas and Propagation (EuCAP)*, 2022.